μ-1,2-Peroxobridged di-iron(III) dimer formation in human H-chain ferritin

Fadi BOU-ABDALLAH*, Georgia C. PAPAEFTHYMIOU†, Danielle M. SCHESWOHL†, Sean D. STANGA†[1], Paolo AROSIO‡ and N. Dennis CHASTEEN*[1]

*Department of Chemistry, University of New Hampshire, Durham, NH 03824, U.S.A., †Department of Physics, Villanova University, Villanova, PA 19085, U.S.A., and ‡Chemistry Section, Faculty of Science, University of Brescia, 25123 Brescia, Italy

Biomineralization of the ferritin iron core involves a complex series of events in which H_2O_2 is produced during iron oxidation by O_2 at a dinuclear centre, the 'ferroxidase site', located on the H-subunit of mammalian proteins. Rapid-freeze quench Mössbauer spectroscopy was used to probe the early events of iron oxidation and mineralization in recombinant human ferritin containing 24 H-subunits. The spectra reveal that a μ-1,2-peroxodiFe(III) intermediate (species P) with Mössbauer parameters δ (isomer shift) = 0.58 mm/s and ΔE_Q (quadrupole splitting) = 1.07 mm/s at 4.2 K is formed within 50 ms of mixing Fe(II) with the apoprotein. This intermediate accounts for almost all of the iron in the sample at 160 ms. It subsequently decays within 10 s to form a μ-oxodiFe(III)–protein complex (species D), which partially vacates the ferroxidase sites of the protein to generate Fe(III) clusters (species C) at a reaction time of 10 min. The intermediate peroxodiFe(III) complex does not decay under O_2-limiting conditions, an observation suggesting inhibition of decay by unreacted Fe(II), or a possible role for O_2 in ferritin biomineralization in addition to that of direct oxidation of iron(II).

Key words: iron biomineralization, Mössbauer spectroscopy, peroxo iron(III) complex, rapid-freeze quench.

INTRODUCTION

The mechanism of oxidative deposition of iron within the iron storage protein ferritin has been the subject of intense investigation for many years [1–3]. The 24 subunits constituting the protein shell of mammalian ferritins are of two types, H and L, having molecular masses of approx. 21000 and 20000 Da respectively. Iron(II) is oxidized at a dinuclear ferroxidase centre located on the H-subunit of the protein [3,4]. The L-subunit lacks such a centre, and appears to be largely involved in mineralization of the hydrous ferric oxide core within the interior of the protein shell [5]. The mineral core is the ultimate thermodynamic sink for the iron acquired by the protein.

It is well established that hydrogen peroxide is a product of dioxygen reduction in H-chain ferritins [6–9]. The dinuclear iron centre located on this subunit seems structurally well suited to carry out the required two electron reduction of O_2 to produce H_2O_2, possibly via formation of a peroxodiFe(III) intermediate at this centre. A number of previous studies have been directed at identifying such an intermediate. In early stopped-flow studies of iron oxidation in H-chain bullfrog ferritin (BfHF), a purple intermediate ($\lambda_{max} \approx 550$ nm) was observed; however, on the basis of resonance Raman spectroscopy, it was assigned to a transient Fe(III)-tyrosinate complex [7,10] rather than to a peroxodiFe(III) intermediate. Subsequent Mössbauer spectroscopic studies of rapid-freeze quenched samples of BfHF similarly failed to detect a peroxo complex [11], although oximetry measurements have shown that H_2O_2 is produced during iron(II) oxidation in this protein [7].

In contrast with BfHF, stopped-flow kinetics studies of human H-chain ferritin (HuHF) have revealed a different intermediate having a blue colour ($\lambda_{max} \approx 650$ nm) that is formed within 0.14 s of mixing Fe(II) and the apoprotein in the presence of O_2 [12]. This intermediate subsequently decayed over a period of about 10 s [12]. No coloured intermediate was observed in stopped-flow measurements with *Escherichia coli* bacterioferritin (EcBFR) [13], whereas an intermediate ($\lambda_{max} \approx 600$ nm) was seen with *E. coli* ferritin type A (EcFtnA), but of lower absorption intensity than for HuHF [12,14]. Measurements with various site-directed mutants of EcFtnA have excluded the intermediate species from being an Fe^{3+}-tyrosinate complex or a tryptophan radical. Instead, the 600 nm, and 650 nm, absorption bands of EcFtnA and HuHF respectively, have been attributed to peroxodiFe(III) intermediates in these proteins [14]. Their absorption spectra have some similarities to those of the known peroxo bridged di-iron(III) centres of the R2 subunit of ribonucleotide reductase (RNR) [15], methane mono-oxygenase (MMO) [16], stearoyl-ACPΔ^9-desaturase [17] and model complexes [18].

Recent work with bullfrog M-subunit ferritin (BfMF) has likewise revealed a transient absorption at 650 nm, similar to that of the blue intermediate of HuHF [19]. The kinetics of formation and decay of this intermediate have been studied in detail by a combination of stopped-flow spectrophotometry, rapid-freeze quench Mössbauer spectroscopy and EXAFS [19–22]. This carefully executed work has firmly established that the transient blue complex in BfMF is a μ-1,2-peroxodiferric species located at the ferroxidase centre of this protein. The Mössbauer and resonance Raman spectroscopic signatures of the intermediate [20,21] in conjunction with the EXAFS data [22] have provided insight into its detailed structure.

To date BfMF is the only ferritin where a peroxo intermediate has been unequivocally demonstrated. Since the ferroxidase site ligands of BfMF, HuHF and BfHF are conserved among the three proteins (Figure 1), one would anticipate the same behaviour in their iron oxidation mechanisms, but that is not observed. While both of the H-chain proteins, HuHF and BfHF, produce H_2O_2, only HuHF exhibits an absorption at 650 nm, postulated as that of a peroxo Fe(III) complex [14]. Obviously other protein structural features beside the immediate ligands to the iron play some role in governing the kinetics observed. The

Abbreviations used: BfHF, H-subunit bullfrog ferritin; BfMF, bullfrog M-subunit ferritin; EcBFR, *Escherichia coli* bacterioferritin; EcFtnA, *E. coli* bacterial ferritin type A; HuHF, human H-subunit ferritin; MMO, methane mono-oxygenase; RNR, ribonucleotide reductase.

[1] To whom correspondence should be addressed (e-mail ndc@cisunix.unh.edu).

© 2002 Biochemical Society

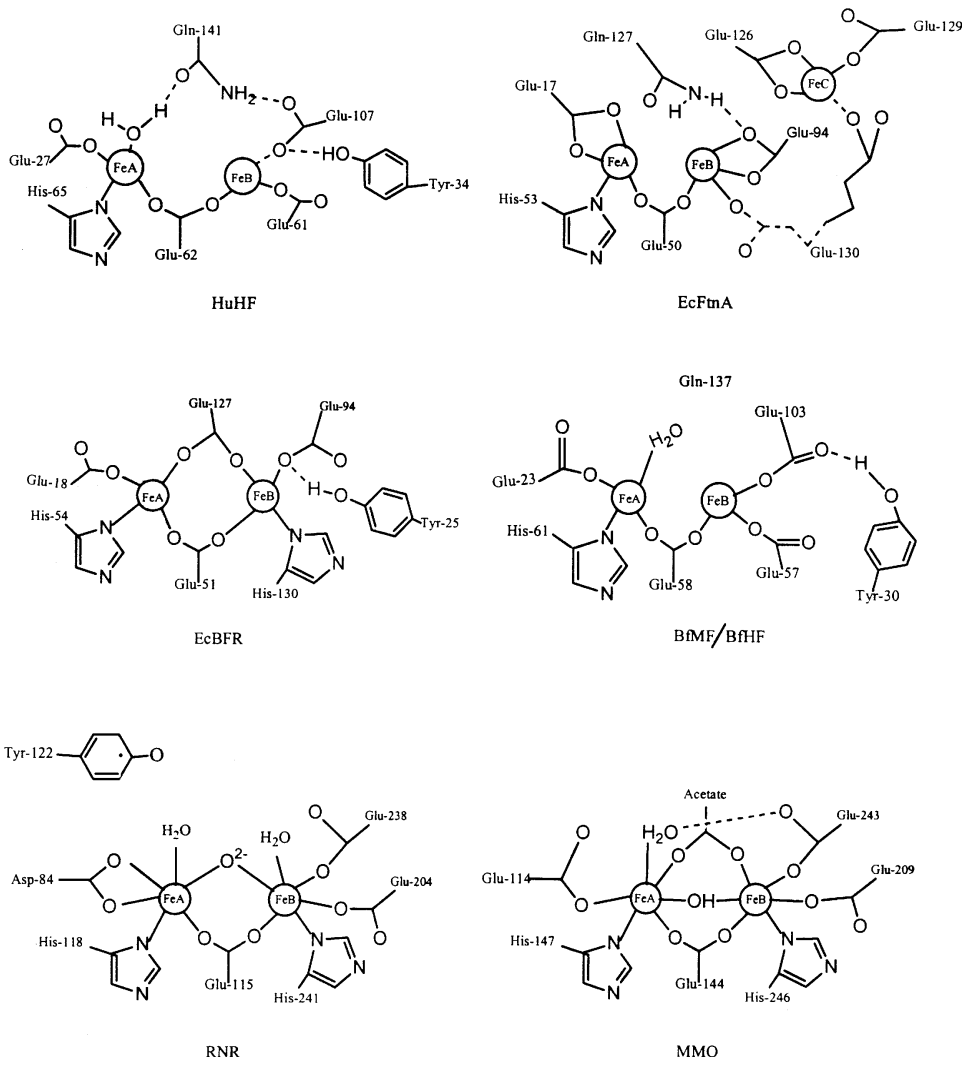

Figure 1 Schematic representation of the dinuclear centres of HuHF, EcFtnA, EcBFR, BfMF/BfHF, RNR and MMO

The structure of BfMF/BfHF is by analogy to that of HuHF [20], with the corresponding amino acids of the amphibian proteins indicated [2]. The structures were constructed using the ChemDraw chemical structure drawing program (CambridgeSoft Corp., Cambridge, MA, U.S.A.).

dissimilar kinetics and coloured intermediates seen in bullfrog H and M proteins, despite the conservation of the ferroxidase ligands, emphasize this point [19]. In the case of bacterioferritin (EcBFR), where some of the protein ligands of the ferroxidase centre differ from those of the other ferritins (Figure 1), water is the final product of dioxygen reduction [23] and no coloured intermediate has been detected [13].

Given the rather large variation seen in the absorption wavelength maximum ($\lambda_{max} \approx 470$–$700$ nm) and intensity ($\epsilon \approx 190$–$3500\ cm^{-1} \cdot M^{-1}$) of peroxodiferric model complexes, dinuclear iron proteins and ferritins (reviewed in [20]), optical spectral data alone are insufficient to establish unequivocally the presence of peroxo species. We have, therefore, undertaken Mössbauer measurements to look for corroborative evidence for peroxo intermediate formation in the mammalian ferritins, as found for the amphibian M-chain protein [19–22].

In the present study, we have employed rapid-freeze quench Mössbauer spectroscopy to examine the blue intermediate ($\lambda_{max} = 650$ nm) previously seen in mammalian H-chain ferritin (HuHF) by stopped-flow spectrophotometry [12]. Following rapid mixing of the apoHuHF with $^{57}Fe(II)$, samples were quickly frozen at -130 °C in an 2-methylbutane bath. The blue, crystalline frozen samples of HuHF exhibited a Mössbauer spectrum characteristic of a diFe(III) peroxo complex, confirming the assignment by Harrison and coworkers [14] on the basis of its optical spectrum. Thus peroxobridged complex formation has now been established for a mammalian ferritin and may, indeed, be a common intermediate of all ferritins which exhibit an $Fe:O_2$ oxidation stoichiometry of 2:1 and which produce H_2O_2 as a product of dioxygen reduction. In addition, evidence for ferrous binding to HuHF before peroxo complex formation is presented. A μ-oxobridged Fe(III) dimer is formed following decay of the peroxo intermediate, ultimately leading to Fe(III) clusters.

EXPERIMENTAL

Recombinant human H-chain ferritin was prepared as described previously [24]. The protein concentration was determined by the absorbance at 280 nm ($\epsilon = 23000\ M^{-1} \cdot cm^{-1}$/subunit) [9].

© 2002 Biochemical Society

The protein was rendered iron free by continuous flow anaerobic ultrafiltration using dithionite and 1,2-bipyridyl [25]. The $^{57}FeSO_4$ solution was typically prepared by dissolving 0.71 mg of iron-57 metal (95.1 atom%; U.S. Service, Inc., Summit, NJ, U.S.A.) in 100 μl of 0.146 M H_2SO_4 (10%, v/v) over a period of 4 days, followed by dilution with 850 μl of water to produce a final solution of 0.0131 M $FeSO_4$ at pH 2. An Update Instrument System 1000 freeze-quench apparatus was used to prepare the samples for Mössbauer spectroscopy. The protein concentrations before mixing were 81.9 or 136 μM in an aqueous solution of 0.10 or 0.15 M Mes buffer, pH 6.7, for the 40 Fe/shell or 24 Fe/shell samples respectively.

The protein and iron solutions were loaded in 2 ml and 0.5 ml syringes respectively, pushed in a 4:1 ratio through the mixer and reactor (ageing) hose and sprayed into a funnel containing 2-methylbutane immersed in the quench bath maintained at −130 °C. The reactor hose was flushed with argon gas before use to minimize uptake of additional O_2 by the Fe(II)–apoferritin solution following mixing. The stated concentrations of all components described in the Figure legends are those following mixing, and the pH was 6.5. The 'dead time' of our instrument was 15 ms [26]. The temperature of the 2-methylbutane was monitored with a copper constantan thermocouple, and maintained by adding liquid nitrogen to the outer jacket of the quench bath. The device used to collect the 1 ml Mössbauer sample was a modified design of one described previously [27]. (Engineering drawings of the device are available from our laboratory upon request.) After spraying the sample into the funnel containing cold 2-methylbutane, the sample was allowed to stand for 20–30 min, allowing the crystals to settle. The sample was then carefully but firmly packed in the Mössbauer cup. The funnel was removed from the packing shaft and the liquid 2-methylbutane was decanted. The packing shaft with the cup attached was then quickly placed in a 254-mm-tall ground glass holder pre-chilled in dry ice (−78 °C), and was subsequently evacuated to remove all liquid 2-methylbutane entrained within the sample. The cup was finally detached from the packing shaft using chilled pliers, and the top was put in place using tweezers and a small screwdriver. The lid of the Mössbauer cup had a 0.5-mm-diameter hole to vent gases during the cryogenic experiments. During sample handling, the Mössbauer cup was kept in contact with powdered dry ice. Samples were shipped overnight on dry ice, and stored in liquid nitrogen before the Mössbauer experiments.

Mössbauer measurements were performed using a constant acceleration Ranger Electronics Mössbauer spectrometer. Data were stored in an MCS-32 EG&G Ortec multiscaler card installed in a Hewlett–Packard Pentium II computer. The spectrometer was calibrated with a thin iron foil enriched in ^{57}Fe. The source was 25 mCi of ^{57}Co in rhodium maintained at room temperature. Low sample temperatures were achieved with a Janis Research Co. Supervaritemp cryogenic dewar. Temperatures above that of liquid helium were maintained to within ±0.2 K using a Lakeshore Cryotronics (Westerville, OH, U.S.A.) temperature controller. Mössbauer spectra were fitted using the least-squares method to theoretical models, assuming Lorentzian line shapes using the WMOSS fitting software of Web Research Corporation.

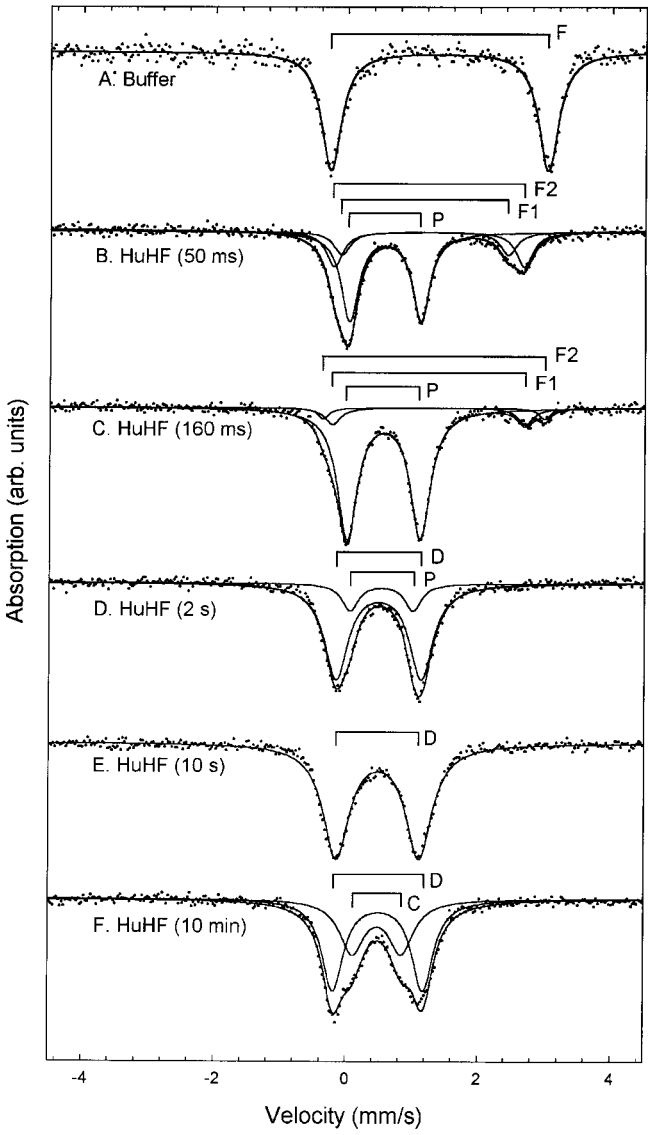

Figure 2 Mössbauer spectra of HuHF samples frozen at various times under a 100% O_2 atmosphere

Conditions: 2.62 mM ^{57}Fe in 0.12 M Mes buffer, pH 6.5, and at 120 K. Traces: (**A**), buffer only; (**B**), 24 Fe/protein and 109 μM protein; (**C**–**F**), 40 Fe/protein and 65.5 μM protein.

RESULTS AND DISCUSSION

Freeze-quench Mössbauer spectra were measured from samples where the protein solutions before rapid mixing were pre-equilibrated under an atmosphere of either 100% O_2 (Figure 2) or 21% O_2 (Figure 3), and the Fe(II) solution under an atmosphere of 21% O_2. Since the reaction stoichiometry is 2 Fe(II)/O_2, the 100% O_2 samples contained sufficient dissolved O_2 (1.12 mM) to essentially oxidize all of the 2.62 mM Fe(II) in the mixed solution, whereas the 21% O_2 samples were oxygen-deficient. The Mössbauer parameters obtained from curve-fitting the families of spectra in Figures 2 and 3, measured at 120 K and 4.2 K respectively, as well as spectra for other samples not shown, are summarized in Table 1. Since little difference was observed between spectra obtained at 4.2 and 120 K (Table 1), spectra obtained in the latter stages of this work were measured at 120 K to conserve liquid helium. Identification of the various species generated during the time course of the reaction is on the basis of the published assignments from previous work on a number of ferritins [11,20,25,28–31]. The percentages of species

© 2002 Biochemical Society

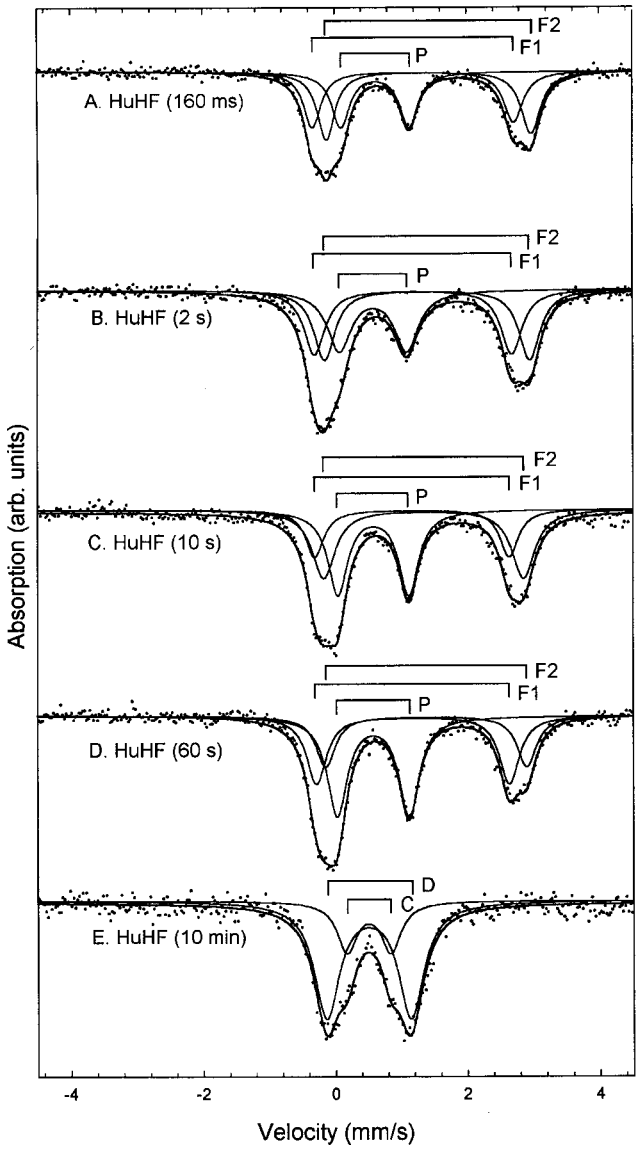

Figure 3 Mössbauer spectra of HuHF samples frozen at various times under a 21% O_2 atmosphere

Conditions: 40 Fe/protein, 65.5 μM protein, 2.62 mM ^{57}Fe in 0.08–0.12 M Mes buffer, pH 6.5, at 4.2 K.

Table 1 Mössbauer parameters of HuHF

Errors in the last digits (as S.D. of the mean values shown) of the isomer shift (δ), quadrupole splitting (ΔE_Q) and line width (LW) parameters are given in parentheses.

	Parameter			
Species	δ (mm/s)	ΔE_Q (mm/s)	LW (mm/s)	T (K)
Fe (II) in buffer (F)	1.39 (1)	3.29 (1)	0.37 (1)	4.2
	1.39 (1)	3.30 (1)	0.36 (1)	120
Fe(II) complex #1 (F1)	1.17 (3)	2.99 (6)	0.32 (6)	4.2
Fe(II) complex #2 (F2)	1.41 (3)	3.08 (6)	0.34 (6)	4.2
Fe(III) peroxodimer (P)	0.58 (1)	1.07 (1)	0.37 (1)	4.2
	0.55 (1)	1.11 (1)	0.37 (1)	120
Fe(III) oxodimer (D)	0.50 (3)	1.30 (6)	0.45 (6)	4.2
	0.48 (1)	1.26 (1)	0.48 (1)	120
Fe(III) cluster (C)	0.51 (3)	0.70 (6)	0.39 (6)	4.2
	0.48 (3)	0.74 (6)	0.39 (6)	120

Table 2 Percentages of species as a function of quench time for 100% O_2 samples

Measurements were made at a temperature of 120 K. Errors in the last digit (as S.D. of the mean values shown) are given in parentheses. The $t = 10$ min samples were thawed and stirred in air.

Time	Fe(II) complexes (F1 plus F2)	Fe(III) peroxo dimer (P)	Fe(III) oxo dimer (D)	Cluster (C)
50 ms	38 (2)	62 (2)	–	–
160 ms	13 (5)	87 (2)	–	–
2 s	–	37 (5)	63 (5)	–
10 s	–	–	100 (2)	–
10 min	–	–	60 (5)	40 (5)

Table 3 Percentages of species as a function of quench time for 21% O_2 samples

Measurements were performed at 4.2 K. Errors in last digit (as S.D. of the mean values shown) are given in parentheses. The $t = 10$ min samples were thawed and stirred in air.

Time	Fe(II) complex #1 (F1)	Fe(II) complex #2 (F2)	Fe(III) peroxo dimer (P)	Fe(III) oxo dimer (D)	Cluster (C)
160 ms	27 (5)	42 (5)	31 (2)	–	–
2 s	31 (5)	37 (5)	32 (2)	–	–
10 s	36 (5)	25 (5)	39 (2)	–	–
60 s	40 (5)	15 (5)	45 (2)	–	–
10 min	–	–	–	70 (5)	30 (5)

observed as a function of time are summarized in Tables 2 and 3 for the 100% and 21% O_2 atmosphere samples respectively.

Figure 2(A) shows the spectrum obtained when Fe(II) is shot into buffer and frozen at 160 ms. The characteristic quadrupole doublet of a high-spin Fe(II) buffer species designated F is evident [isomer shift (δ) = 1.39 mm/s and quadrupole splitting (ΔE_Q) = 3.29 mm/s; Table 1]. In contrast with the buffer, the 100% O_2 samples of HuHF at 50 and 160 ms (Figures 2B and 2C) show pronounced oxidation, with the appearance of a quadrupole doublet of an Fe(III) species designated 'P' having parameters $\delta = 0.55 \pm 0.01$ mm/s and $\Delta E_Q = 1.11 \pm 0.01$ mm/s at 120 K. Similar parameters are obtained at 4.2 K (Table 1). The 50 and 160 ms frozen protein samples of Figure 2 were intensely blue in colour, whereas the buffer sample was white.

The isomer shift ($\delta = 0.58 \pm 0.01$ mm/s) and quadrupole splitting ($\Delta E_Q = 1.07 \pm 0.01$ mm/s) parameters of the Fe(III) species P of HuHF at 4.2 K are strikingly similar to those of the well-characterized μ-1,2-peroxodiferric centre of the amphibian M-chain protein at this temperature ($\delta = 0.62 \pm 0.02$ mm/s; $\Delta E_Q = 1.08 \pm 0.03$ mm/s) [19–22]. The parameters are also similar to those of the dinuclear iron centre of MMO ($\delta = 0.66$ mm/s; $\Delta E_Q = 1.51$ mm/s)[32] and those of the Asp$^{84} \rightarrow$ Glu variant of the R2 subunit of RNR ($\delta = 0.63$ mm/s; $\Delta E_Q = 1.58$ mm/s) [15]. These latter proteins exhibit larger quadrupole splittings, which presumably reflect the differences among the protein ligands of these enzymes and those of the ferritins. Most notably, RNR and MMO contain an additional histidine residue in co-ordination

© 2002 Biochemical Society

positions that are occupied by glutamate ligands in HuHF and have different bridging structures (Figure 1) [3,33,34].

At 50 and 160 ms under a 100 % atmosphere, only the μ-1,2-peroxodiFe(III) complex (species P) and unoxidized Fe(II) species (F1 and F2) are observed (Figure 2 and Table 2). The differences in the Fe(II) Mössbauer parameters between the buffer and protein samples (Figures 2A, 2B and 2C, and Table 1) imply that the ferrous ion binds to the protein within the reaction time of 50 ms. This finding is consistent with multi-mixing, stopped-flow kinetic data, suggesting that Fe(II) binding to HuHF is complete within 50 ms [35]. Fe(II) appears to be present in two forms in the protein, Fe(II) complexes #1 and #2 (Table 1), designated 'F1' and 'F2' in Figure 2. Their signals are more pronounced in the spectra of the 21 % O_2 sample shown in Figure 3 (see below).

To look for possible formation of early mononuclear Fe(III) species at the ferroxidase sites, the sample at 50 ms was prepared with 24 Fe/protein to half-saturate the ferroxidase sites. Only the peroxo complex and unoxidized Fe(II) was observed (Figure 2B), implying that, if present, mononuclear Fe(III) or other early species must be formed in low amounts (< 10 % of the total). Thus the present Mössbauer data provide no evidence for the stepwise oxidation of the two Fe(II) ions of the ferroxidase site.

At 160 ms and 100 % O_2, the peroxo species accounted for nearly all of the iron present (Table 2), a time corresponding to that for maximum colour development observed in the stopped-flow experiment [12]. At a quench time of 2 s, a second iron(III) species appeared, designated 'D' in Figure 2(D). This species is assigned to a μ-oxobridged diFe(III) complex at the ferroxidase site (Tables 1 and 2), with parameters similar to those of a μ-oxodiFe(III) dimer ($\delta = 0.50 \pm 0.01$ mm/s; $\Delta E_Q = 1.23 \pm 0.01$ mm/s) reported previously for HuHF for reaction times $\geqslant 30$ s [28]. The sample was completely bleached by 10 s, as also observed by stopped-flow spectrophotometry [12], and only the oxobridged diFe(III) dimer remained (Figure 2E; Table 2). By this time, H_2O_2 is presumably released into solution.

The 10 s sample was thawed, stirred and refrozen at 10 min (Figure 2F). In addition to the μ-oxo dimer D, a new species appeared and was assigned to an Fe(III) cluster, C, representing 40 % of the total iron. The cluster is presumably derived from dimer D (Table 2). The value of 40 % cluster formation correlates well with the expected percentage of ferroxidase sites vacated after 10 min at pH 6.5, as observed by oximetry studies [8]. Thus the Mössbauer spectra report on the clearance reaction of the ferroxidase site.

Previous studies of recombinant human H-chain ferritins have shown the formation of large superparamagnetic clusters, as well as of a slowly relaxing monomeric iron species at longer reaction times of 20 or 30 min [28]. These species are not readily observed in our samples prepared at the shorter time of 10 min. The absence of a magnetic hyperfine sextet in our 4.2 K spectra at a 10 min reaction time indicates that the majority of clusters formed within the protein shell are small, possessing blocking temperatures below 4.2 K. The magnetic signature of a small percentage of superparamagnetic clusters with blocking temperatures above 4.2 K would be difficult to distinguish above the noise level of the spectrum. However, the percentage of doublet C from clusters decreased from 40 % at 120 K to 30 % at 4.2 K for the same sample (results not shown), providing indirect evidence for the presence of a small amount (≈ 10 %) of larger superparamagnetic clusters. Similarly, hyperfine sextets from small amounts of reported slowly relaxing monomeric Fe(III) species [28] would also have been difficult to observe with our samples.

The 21 % O_2 spectra in Figure 3 show, in addition to the peroxo complex P, the presence of substantial amounts of unoxidized Fe(II) resulting from insufficient O_2 in the solution. At 160 ms, the peroxo complex accounted for only 31 % of the iron, slowly increasing to 45 % by a reaction time of 60 s (Figure 3 and Table 3). Significantly, the peroxodiFe(III) complex does not decay under conditions of oxygen limitation, suggesting an additional function for O_2 as a facilitator of peroxo complex decay or an inhibition of decay by unoxidized Fe(II) bound to the protein. It was not until the sample was thawed and stirred in air for 10 min that the peroxo complex disappeared, and was replaced by a composite spectrum comprising the oxodimer D and cluster C (Figure 3E), as also seen for the 100 % O_2 sample (Figure 2F).

It is also noteworthy that the amount of Fe(II) oxidized in the 21 % O_2 sample exceeds that expected from the amount of O_2 in solution by approximately a factor of 2, assuming a 2 Fe(II):O_2 reaction stoichiometry. Although the ageing hose in the freeze-quench apparatus was flushed with argon, some further uptake of O_2 by the solution following mixing might have occurred. Alternatively, oxidizing equivalents might be associated with the protein itself in the form of bound O_2, which contribute to the total amount of Fe(II) undergoing oxidation. These unexplained O_2 phenomena are beyond the scope of the present study, however, and will be the subject of future research.

It is also apparent from the data in Table 3, that the distribution of iron between Fe(II) species #1 and #2 changes in time. The percentages of Fe(II) species #1 and the peroxo complex increase, while Fe(II) species #2 decreases, with time. Fe(II) species #2 might represent iron at an initial Fe(II) binding site on ferritin which then migrates to the ferroxidase site to produce species #1. It seems unlikely that these two species represent the two sites of the ferroxidase centre, since in this case they would be expected to be consumed at the same rate during formation of the peroxo complex, but they are not. Alternatively, the two Fe(II) species #1 and #2, might be associated with two slightly different, transient protein conformational states, that may arise due to O_2 proximity at the ferroxidase site, but before peroxo complex formation at the dinuclear centre.

The Fe(II) species #1 and #2 seen in the present work have somewhat different Mössbauer parameters than those of the two ferrous species previously reported at a quench time of 1 min for the ferroxidase-centre variant $Glu^{27} \rightarrow Ala$ of HuHF ($\delta = 1.21 \pm 0.01$ mm/s and $\Delta E_Q = 2.78 \pm 0.01$ mm/s, and $\delta = 1.31 \pm 0.01$ mm/s and $\Delta E_Q = 3.26 \pm 0.01$ mm/s, at 4.1 and 90 K respectively in a 21 % O_2 atmosphere) [28], implying that there might be other iron(II) binding sites on the protein that become observable when the ferroxidase centre is disabled and longer quench times are employed. Alternatively, mutagenesis might alter the structure of the Fe(II) binding sites on the protein. The identity and functionality of the ferrous-binding sites are major unanswered questions in ferritin chemistry.

The present work establishes that the 650 nm absorption in HuHF results from a μ-1,2-peroxodiFe(III) complex, as postulated previously [14] and as established for BfMF [19–22]. The other ferritin with a coloured intermediate, EcFtnA ($\lambda_{max} \approx 600$ nm), has not been examined by freeze-quench Mössbauer spectroscopy. However, the mechanism of iron oxidation in EcFTnA might also proceed via a peroxo intermediate, as proposed by Zhao et al. [14]. In contrast, the lack of a transient absorption close to 650 nm, for EcBFR [13] might be due to its different binuclear centre. Both irons are co-ordinated by a histidine residue in EcBFR, and there is an additional bridging carboxylate group (Figure 1). In connection with this, the novel 12-subunit ferritin from *Listeria innocua* also reduces O_2 to H_2O [36], and its ferroxidase site is richer in histidine ligands than vertebrate ferritins [37]. Whether peroxodiFe(III) complexes are formed in

© 2002 Biochemical Society

these bacterial proteins is at present unknown. As reported by others [20], the failure to observe a peroxo complex in the amphibian H-chain ferritin, whereas one is seen in the M-chain protein, might be because its concentration is too low to be observed spectroscopically. The key protein ligands of the ferroxidase site are conserved between BfHF and BfMF (Figure 1), so peroxo complex formation is anticipated in both proteins [2]. Detection of the peroxo intermediate in RNR initially proved difficult ([15], and references therein).

In conclusion, the present work has confirmed and extended previous Mössbauer and stopped-flow studies of the oxidative deposition of iron in human H-chain ferritin. Specifically, formation of a peroxodiFe(III) complex has been confirmed independently, and an apparent O_2 requirement for its decay observed for the first time. The overall sequence for iron oxidation and mineralization follows the general pattern: free Fe(II) → Fe(II)–protein complexes → peroxodiFe(III)–protein complex → oxodiFe(III)–protein complex → small Fe(III) cluster → large Fe(III) cluster. Formation of other intermediate species, such as mononuclear Fe(III) and radical species as suggested by other research groups previously [26,28], is not precluded by the present data.

This work was supported by grant R37 GM20194 from the National Institute of General Medical Sciences (N.D.C.), by the Italian Ministry of the University and Scientific and Technologic Research (MURST) Cofin-99 (P.A.) and by CNR, Targeted Project in Biotechnology (P.A.) and by the National Science Foundation, grant DMR-0074537 (G.C.P.). We thank Ms Christine Janus-Chandler for preparing the recombinant human H-chain ferritin, and Dr Arthur Viescas for technical support. D.M.S. and S.D.S. thank the Howard Hughes Medical Institute (HHMI) for financial support. D.M.S. and S.D.S. are Howard Hughes Medical Institute Undergraduate Summer Research Scholars at Villanova University.

REFERENCES

1 Chasteen, N. D. and Harrison, P. M. (1999) Mineralization in ferritin: an efficient means of iron storage. J. Struct. Biol. **126**, 182–194
2 Waldo, G. S. and Theil, E. C. (1996) Ferritin and iron biomineralization. In Comprehensive Supramolecular Chemistry (Suslick, K. S., ed.), vol. 5, pp. 65–89, Pergamon Press, Oxford
3 Harrison, P. M. and Arosio, P. (1996) Ferritins: Molecular properties, iron storage function and cellular regulation. Biochim. Biophys. Acta **1275**, 161–203
4 Lawson, D. M., Artymiuk, P. J., Yewdall, S. J., Smith, J. M. A., Livingstone, J. C., Treffry, A., Luzzago, A., Levi, S., Arosio, P., Cesareni, G. et al. (1991) Solving the structure of human H ferritin by genetically engineering intermolecular crystal contacts. Nature (London) **349**, 541–544
5 Levi, S., Yewdall, S. J., Harrison, P. M., Santambrogio, P., Cozzi, A., Rovida, E., Albertini, A. and Arosio, P. (1992) Evidence that H- and L-chains have co-operative roles in the iron uptake mechanism of human ferritin. Biochem. J. **288**, 591–596
6 Xu, B. and Chasteen, N. D. (1991) Iron oxidation chemistry in ferritin: increasing Fe/O_2 stoichiometry during core formation. J. Biol. Chem. **266**, 19965–19970
7 Waldo, G. S. and Theil, E. C. (1993) Formation of iron(III)-tyrosinate is the fastest reaction observed in ferritin. Biochemistry **32**, 13262–13269
8 Yang, X., Chen-Barrett, Y., Arosio, P. and Chasteen, N. D. (1998) Reaction paths of iron oxidation and hydrolysis in horse spleen and recombinant human ferritins. Biochemistry **37**, 9743–9750
9 Zhao, G., Bou-Abdallah, F., Yang, X., Arosio, P. and Chasteen, N. D. (2001) Is hydrogen peroxide produced during iron(II) oxidation in mammalian apoferritins? Biochemistry **40**, 10832–10838
10 Waldo, G. S., Ling, J., Sanders-Loehr, J. and Theil, E. C. (1993) Formation of a Fe(III)–tyrosinate complex during biomineralization of H-subunit ferritin. Science (Washington, D.C.) **259**, 796–798
11 Pereira, A. S., Tavares, P., Lloyd, S. G., Danger, D., Edmondson, D. E., Theil, E. C. and Huynh, B. H. (1997) Rapid and parallel formation of Fe^{3+} multimers, including a trimer, during H-type subunit ferritin mineralization. Biochemistry **36**, 7917–7927
12 Treffry, A., Zhao, Z., Quail, M. A., Guest, J. R. and Harrison, P. M. (1995) Iron(II) oxidation by H chain ferritin: evidence from site-directed mutagenesis that a transient blue species is formed at the dinuclear iron center. Biochemistry **34**, 15204–15213
13 Le Brun, N. E., Wilson, M. T., Andrews, S. C., Guest, J. R., Harrison, P. M., Thomson, A. J. and Moore, G. R. (1993) Kinetic and structural characterization of an intermediate in the biomineralization of bacterioferritin. FEBS Lett. **333**, 197–202
14 Zhao, Z., Treffry, A., Quail, M. A., Guest, J. R. and Harrison, P. M. (1997) The early intermediate is not an iron tyrosinate. J. Chem. Soc. Dalton Trans., 3977–3978
15 Bollinger, Jr., J. M., Krebs, C., Vicol, A., Chen, S., Ley, B. A., Edmondson, D. E. and Huynh, B. H. (1998) Engineering the diiron site of *Escherichia coli* ribonucleotide reductase protein R2 to accumulate an intermediate similar to Hperoxo, the putative peroxodiiron(III) complex from the methane monooxygenase catalytic cycle. J. Am. Chem. Soc. **120**, 1094–1095
16 Liu, K. E., Valentine, A. M., Qiu, D., Edmondson, D. E., Appelman, E. H., Spiro, T. G. and Lippard, S. J. (1995) Characterization of a diiron(III) peroxo intermediate in the reaction cycle of methane monooxygenase hydroxylase from *Methylococcus capsulatus* (Bath). J. Am. Chem. Soc. **117**, 4997–4998
17 Broadwater, J. A., Achim, C., Münck, E. and Fox, B. G. (1999) Mössbauer studies of the formation and reactivity of a quasi-stable peroxo intermediate of stearoyl-acyl carrier protein Δ^9-desaturase (Δ9D). Biochemistry **38**, 12197–12204
18 Kitajima, N., Tamura, N., Amagai, H., Fukui, H., Mooro-oia, Y., Mizutani, Y., Kitagway, T., Mathur, R., Heerwegh, K., Reed, C. A. et al. (1994) Monomeric carboxylate ferrous complexes as models for the dioxygen binding sites in non-heme iron proteins. The reversible formation and characterization of μ-peroxo diferric complexes. J. Am. Chem. Soc. **116**, 9071–9085
19 Fetter, J., Cohen, J., Danger, D., Sanders-Loehr, J. and Theil, E. C. (1997) The influence of conserved tyrosine-30 and tissue dependent differences in sequence on ferritin function – use of blue and purple Fe(III) species as reporters of ferroxidation. J. Biol. Inorg. Chem. **2**, 652–661
20 Pereira, A. S., Small, W., Krebs, C., Tavares, P., Edmondson, D. E., Theil, E. C. and Huynh, B. H. (1998) Direct spectroscopic and kinetic evidence for the involvement of a peroxodiferric intermediate during the ferroxidase reaction in fast ferritin mineralization. Biochemistry **37**, 9871–9876
21 Moenne-Loccoz, P., Krebs, C., Herlihy, K., Edmondson, D. E., Theil, E. C., Huynh, B. H. and Loehr, T. M. (1999) The ferroxidase reaction of ferritin reveals a diferric μ-1,2 bridging peroxide intermediate in common with other O_2-activating non-heme diiron proteins. Biochemistry **38**, 5290–5295
22 Hwang, J., Krebs, C., Huynh, B. H., Edmondson, D. E., Theil, E. C. and Penner-Hahn, J. E. (2000) A short Fe–Fe distance in peroxodiferric ferritin: control of Fe substrate versus cofactor decay? Science (Washington, D.C.) **287**, 122–125
23 Yang, X., Le Brun, N. E., Thomson, A. J., Moore, G. R. and Chasteen, N. D. (2000) The iron oxidation and hydrolysis chemistry of *Escherichia coli* bacterioferritin. Biochemistry **39**, 4915–4923
24 Levi, S., Salfeld, J., Franceschinelli, F., Cozzi, A., Dorner, M. H. and Arosio, P. (1989) Expression and structural and functional properties of human ferritin L-chain from *Escherichia coli*. Biochemistry **28**, 5179–5184
25 Bauminger, E. R., Harrison, P. M., Hechel, D., Nowik, I. and Treffry, A. (1991) Mössbauer spectroscopic investigation of structure–function relations in ferritins. Biochim. Biophys. Acta. **1118**, 48–58
26 Sun, S. and Chasteen, N. D. (1994) Rapid kinetics of EPR-active species formed during initial iron uptake in horse spleen apoferritin. Biochemistry **33**, 15095–15102
27 Ravi, N., Bollinger, Jr., J. M., Huynh, B. H., Edmondson, D. E. and Stubbe, J. (1994) Mechanism of assembly of the tyrosyl radical diiron(III) cofactor of *E. coli* ribonucleotide reductase: Moessbauer characterization of the diferric radical precursor. J. Am. Chem. Soc. **116**, 8007–8014
28 Bauminger, E. R., Harrison, P. M., Hechel, D., Hodson, N. W., Nowik, I., Treffry, A. and Yewdall, S. J. (1993) Iron (II) oxidation and early intermediates of iron-core formation in recombinant human H-chain ferritin. Biochem. J. **296**, 709–719
29 Bauminger, E. R., Treffry, A., Quail, M. A., Zhao, Z., Nowik, I. and Harrison, P. M. (1999) Stages in iron storage in the ferritin of *Escherichia coli* (EcFtnA): analysis of Mössbauer spectra reveals a new intermediate. Biochemistry **38**, 7791–7802
30 Bauminger, E. R., Treffry, A., Quail, M. A., Zhao, Z., Nowik, I. and Harrison, P. M. (2000) Metal binding at the active centre of the ferritin of *Escherichia Coli* (EcFtnA). A Mössbauer spectroscopic study. Inorg. Chim. Acta **297**, 171–180
31 Bauminger, E. R., Harrison, P. M., Nowik, I. and Treffry, A. (1989) Mössbauer spectroscopic study of the initial stages of iron-core formation in horse spleen apoferritin: evidence for both isolated Fe(III) atoms and oxo-bridged Fe(III) dimers as early intermediates. Biochemistry **28**, 5486–5493
32 Liu, K. E., Valentine, A. M., Wang, D., Huynh, B. H., Edmondson, D. E., Salifoglou, A. and Lippard, S. J. (1995) Kinetic and spectroscopic characterization of intermediates and component interactions in reactions of methane monooxygenase from *Methylococcus capsulatus* (Bath). J. Am. Chem. Soc. **117**, 10174–10185
33 Rosenzweig, A. C., Frederick, C. A., Lippard, S. J. and Nordlund, P. (1993) Crystal structure of a bacterial non-haem iron hydroxylase that catalyses the biological oxidation of methane. Nature (London) **366**, 537–543

© 2002 Biochemical Society

34 Nordlund, P., Sjöberg, B.-M. and Eklund, H. (1990) Three-dimensional structure of the free radical protein of ribonucleotide reductase. Nature (London) **345**, 593–598

35 Treffry, A., Zhao, Z., Quail, M. A., Guest, J. R. and Harrison, P. M. (1997) Dinuclear center of ferritin: studies of iron binding and oxidation show differences in the two iron sites. Biochemistry **36**, 432–441

36 Yang, X., Chiancone, E., Stefanini, S., Ilari, A. and Chasteen, N. D. (2000) Iron oxidation and hydrolysis reactions of a novel ferritin from *Listeria innocua*. Biochem. J. **349**, 783–786

37 Ilari, A., Stefanini, S., Chiancone, E. and Tsernoglou, D. (2000) The dodecameric ferritin from *Listeria innocua* contains a novel intersubunit iron-binding site. Nat. Struct. Biol. **7**, 38–43

Received 26 October 2001/6 February 2002; accepted 26 February 2002

© 2002 Biochemical Society